Electronic structures of UTSn (T = Ni, Pd) using photoemission spectroscopy

2004 J. Phys.: Condens. Matter 16 3257

(http://iopscience.iop.org/0953-8984/16/18/025)

INSTITUTE OF PHYSICS PUBLISHING JOURNAL OF PHYSICS: CONDENSED MATTER

J. Phys.: Condens. Matter **16** (2004) 3257–3269 PII: S0953-8984(04)73748-0

Electronic structures of UTSn (T = Ni, Pd) using photoemission spectroscopy

J-S Kang[1], S C Wi[1], J H Kim[1], K A McEwen[2], C G Olson[3], J H Shim[4] and B I Min[4]

[1] Department of Physics, The Catholic University of Korea, Puchon 420-743, Korea
[2] Department of Physics and Astronomy, University College London, WCIE 6BT, UK
[3] Ames Laboratory, Iowa State University, Ames, IA 50011, USA
[4] Department of Physics, Pohang University of Science and Technology, Pohang 790-784, Korea

Received 22 December 2003, in final form 16 March 2004
Published 23 April 2004
Online at stacks.iop.org/JPhysCM/16/3257
DOI: 10.1088/0953-8984/16/18/025

Abstract

Electronic structures of UTSn (T = Ni, Pd) have been investigated using photoemission spectroscopy (PES). The extracted U 5f PES spectra of UTSn (T = Ni, Pd) exhibit a broad peak centred at ∼0.3 eV below E_F with rather small spectral weight near $E_F(N_f(E_F))$. The small $N_f(E_F)$ in UTSn is found to be correlated with the T d PES spectra that have a very low density of states (DOS) near E_F. The temperature-dependent high-resolution PES spectra of UTSn provide evidence for the V-shaped reduced metallic DOS near E_F, but they reveal no appreciable changes in their electronic structures across the magnetic phase transition temperatures. Comparison of the measured PES spectra to the LSDA + U band structure calculation shows reasonably good agreement for UPdSn, but not for UNiSn. Therefore, in contrast to the general consensus of the localized U 5f electrons in UTSn (T = Ni, Pd), our finding supports a rather itinerant nature of U 5f electrons for UPdSn, but not for UNiSn.

1. Introduction

Uranium intermetallic compounds often exhibit interesting magnetic behaviour that is neither very localized nor very itinerant. UNiSn and UPdSn are considered to be well localized with small linear specific-heat coefficients [1, 2], $\gamma \approx 18$–28 mJ mol^{-1} K^{-2} and $\gamma \approx 5$ mJ mol^{-1} K^{-2}, respectively, and with large ordered uranium magnetic moments of ∼1.55 μ_B [3] and ∼2 μ_B [4], respectively, which are significantly larger than in other uranium intermetallic systems [1]. Both UNiSn and UPdSn exhibit interesting phase transitions with the antiferromagnetic (AF) ground states. UNiSn displays an AF order below the Néel temperature $T_N \simeq 43$ K, a structural transition [5] from the cubic MgAgAs-type symmetry to the tetragonal symmetry at T_N, and a semiconductor-to-metal (SM) transition around $T_{MI} \sim 55$ K [6, 7]. This multiple phase transition seems to be anomalous because it is an

inverse metal–insulator transition with a gap-opening above T_N and the structural, SM and AF transitions occur concomitantly. UPdSn exhibits either the hexagonal $CaIn_2$-type structure, in which there is disorder between Pd and Sn atoms, or the related GaGeLi-type structure, which allows Pd/Sn ordering [4]. UPdSn also displays two AF transitions with concomitant lattice distortions. UPdSn undergoes an AF transition below $T_N \simeq 37$ K with the orthorhombic magnetic symmetry (phase I), and undergoes another AF transition below $\simeq$25 K with the monoclinic magnetic symmetry (phase II) [8]. Both AF structures in UPdSn are reported to be noncollinear. The resistivity of UPdSn shows a metallic behaviour in the whole temperature range but with a feature of rapid drop below $T_N \simeq 37$ K [1, 2].

The underlying mechanism of the peculiar multiple phase transitions in UNiSn and UPdSn has been investigated extensively [9–11]. A quadrupolar ordered phase based on the crystalline electric field (CEF) level scheme for the localized $5f^2$ (U^{4+}) configuration [9] has been proposed for the phase transitions in UTSn [10], which seems to be consistent with the inelastic neutron scattering data [11]. In contrast, the localized $5f^3$ (U^{3+}) configuration was proposed based on the neutron diffraction data for UPdSn [12, 13]. Some electronic structure calculation for UPdSn supports the localized U $5f^2$ configuration [14], whereas other calculations argue the itinerant character of U 5f electrons in UNiSn [15, 16] and UPdSn [17]. Neither the theoretically predicted electronic structure of UTSn, nor the $5f^2$ configuration of the localized U^{4+} ion, has been verified by photoemission spectroscopy (PES) experiment. Note that the localized magnetic moments, given by Hund's rules without considering the CEF, are very similar for the $5f^3$ configuration (3.62 μ_B) and for the $5f^2$ configuration (3.58 μ_B). So the effective magnetic moment determined from the high-temperature susceptibility data would not be a good criterion for the U 5f electron configurations.

An early resonant photoemission spectroscopy (RPES) study on polycrystalline UTSn samples (T = Ni, Pd, Pt) with a rather poor instrumental resolution [18] did not address the origin of the phase transitions in UTSn. A valence-band and U 4f core-level PES study on polycrystalline UPdSn sample has also been reported [19]. However, the measured surfaces were prepared by scraping or by Ar-ion sputtering, and so the stoichiometry and the cleanliness of the measured sample surfaces were not very reliable. A recent PES study on UNiSn by some of the present authors [20] has found the importance of the on-site Coulomb interaction U between U 5f electrons. Therefore the nature of 5f electrons in UTSn is still controversial.

In order to explore the role of the electronic structures in the phase transitions of UTSn, we have performed RPES measurements of UTSn (T = Ni, Pd) near the U $5d \rightarrow 5f$ absorption edge and determined the partial spectral weight (PSW) distributions of both the U 5f and Ni/Pd d electrons. We have then compared the experimental data to the electronic structure calculation performed in the LSDA+U method (LSDA: local spin-density functional approximation) [21].

2. Experimental and calculational details

UNiSn and UPdSn polycrystalline samples were made by arc melting constituent elements of high purity [20], and annealed for more than one month in order to achieve the proper structures. X-ray diffraction (XRD) measurements, performed at room temperature, revealed no impurity phases for both samples. UNiSn and UPdSn showed the cubic MgAgAs-type structure and the hexagonal $CaIn_2$-type structure, respectively. Our magnetization measurements showed clear antiferromagnetic transitions in agreement with previous results [6, 8].

Photoemission experiments were carried out at the Ames/Montana ERG/Seya beam-line at the Synchrotron Radiation Center. The details of the PES experiment are the same as those described in [20]. Samples were cooled down to $T_{msr} \lesssim 15$ K and fractured in vacuum with a base pressure better than 3×10^{-11} Torr. The cleanliness of the cleaved surfaces was checked

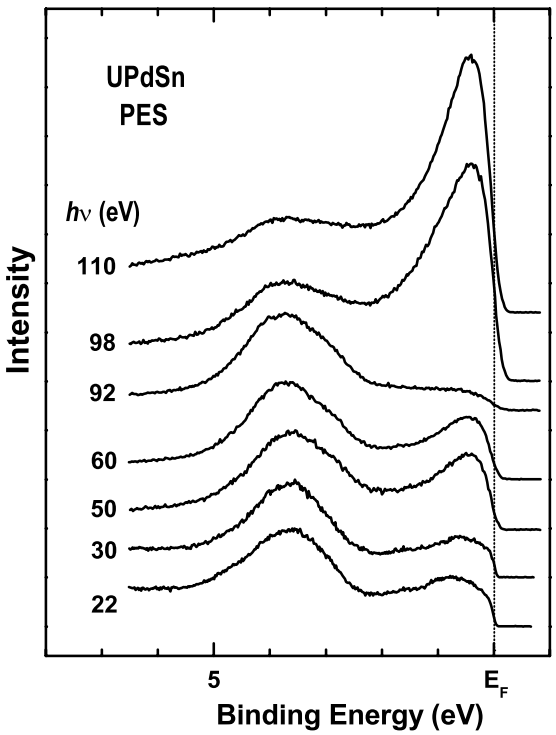

Figure 1. Normalized valence-band spectra of UPdSn. The $h\nu = 22$ and 30 eV spectra are arbitrarily scaled to show their line-shapes better.

by the absence of the 6 eV peak, which is representative of the oxygen contamination of the measured surface. The total instrumental resolution (FWHM: full width at half maximum) was about 80 and 250 meV at $h\nu \sim 20$ and $h\nu \sim 100$ eV, respectively. High resolution photoemission spectra were taken with the FWHM of about 30 meV. The photon flux was monitored by the yield from a gold mesh and all the spectra reported were normalized to the mesh current. Temperature (T)-dependence of PES was also investigated below and above the AF transition temperature. For T-dependent PES measurements, the chamber pressure stayed below 7×10^{-11} Torr during heating. The low-T PES spectra were reproduced after the heating–cooling cycle.

The electronic structures of UTSn have been calculated by employing the self-consistent LMTO (linearized muffin-tin-orbital) band method. The partial densities of states (PDOS) have been calculated by using the LSDA + U band method incorporating the spin–orbit (SO) interaction, so that the orbital polarization is properly taken into account [22]. The von Barth–Hedin form of the exchange–correlation potential has been utilized.

3. Results and discussion

3.1. U 5f and T d PSWs

Figure 1 shows the valence-band spectra of UPdSn in the photon energy ($h\nu$) range of 22–110 eV. The general trend of the $h\nu$-dependence of the valence-band spectrum of UPdSn is very similar to that for UNiSn (see figure 1 in [20]). At low $h\nu$ (22–30 eV), the contribution

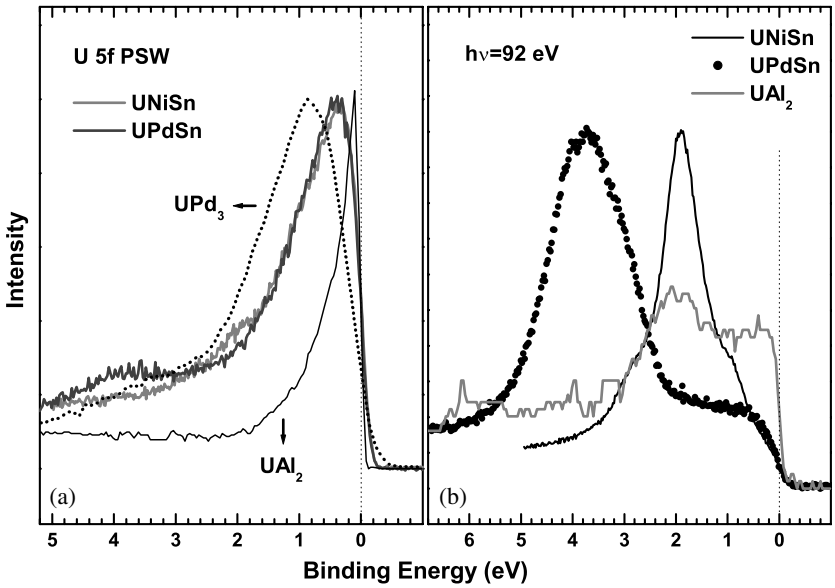

Figure 2. (a) Comparison of the U 5f PSWs of UTSn (T = Ni, Pd), UAl_2 [28] and UPd_3 [27]. (b) Comparison of the off-resonance spectra ($h\nu = 92$ eV) of UTSn (T = Ni, Pd) and UAl_2 [28].

from the Sn sp electron emission is non-negligible (10–15%), and the cross-sections (σ) of U 6d and Pd d electrons are comparable to one another (∼40%) [23]. The U 5f photoemission intensity is enhanced due to the U 5d → 5f resonance effect through the interference between two processes [24, 25]. The first is the direct valence-band photoemission process of

$$5d^{10}5f^{n} + h\nu \rightarrow 5d^{10}5f^{n-1}\epsilon_k, \tag{1}$$

where ϵ_k denotes the emitted electron, and the second process corresponds to the 5d core-hole absorption into intermediate excited states, followed by a two-electron super Coster–Kronig Auger decay, such as

$$5d^{10}5f^{n} + h\nu \rightarrow 5d^{9}5f^{n+1} \rightarrow 5d^{10}5f^{n-1}\epsilon_k. \tag{2}$$

This RPES technique has been applied successfully to enhance the U 5f electron emission [26–28]. $h\nu = 92$, $h\nu = 98$ and $h\nu = 110$ eV correspond to the off- and on-resonance energies due to the U $5d_{5/2} \rightarrow 5f$ and U $5d_{3/2} \rightarrow 5f$ absorptions, respectively [20]. Therefore the emission enhanced at $h\nu = 98$ and 110 eV can be identified as the U 5f emission. The off-resonance spectrum at $h\nu = 92$ eV is dominated by the Pd d emission because, at this $h\nu$, the Sn sp electron emission is negligible with respect to the Pd d emission (<1% of the Pd d emission) and the U 5f emission is suppressed. Using the U 5d → 5f RPES, we have determined the U 5f PSW of UPdSn. Before subtraction, the off-resonance spectrum has been multiplied by a factor of 0.6, in order to account for the $h\nu$-dependence of other conduction-band electrons [23].

Figure 2(a) compares the extracted 5f PSW of UPdSn to those of UNiSn [20], a nearly heavy fermion system UAl_2 [28], and a typically localized 5f system UPd_3 [27]. All the spectra are scaled at the peak. UPd_3 is known to be a tetra-valent (U^{4+}) intermetallic uranium compound with a localized $5f^2$ configuration, and so the 5f peak in UPd_3 is assigned as the $5f^2 \rightarrow 5f^1$ transition [27]. On the other hand, 5f electrons in UAl_2 are expected to be itinerant, and so the 5f peak close to E_F in UAl_2 is considered to represent the fully relaxed $5f^n c^{m-1}$ final states ($n = 2, 3, 4$) under the assumption of the $5f^n c^m$ mixed ground-state configurations.

Interestingly the extracted U 5f spectra of UNiSn and UPdSn are very similar to each other, even though the on- and off-resonance spectra are very different (see figure 1 in this paper and figure 1 in [20]). They have common features, such as a pronounced peak centred at about 0.3 eV binding energy (BE) and a tail to about 3 eV below E_F. It is found that, as one moves from UAl_2 to UTSn and UPd_3, the centroid of the 5f electron peak moves away from E_F and its width becomes wider. This trend is accompanied by the decreasing 5f spectral weight at the Fermi level, $N_f(E_F)$. Compared to the large 5f spectral weight near E_F in UAl_2, $N_f(E_F)$ in UTSn is lower than that in UAl_2, suggesting that U 5f electrons in UTSn are more localized than in UAl_2. This finding is consistent with the fact that UNiSn and UPdSn have large ordered magnetic moments (1.55–2 μ_B) [3, 4], as compared to UAl_2, which is known to be an exchange-enhanced paramagnetic system [29].

There are some uncertainties in determining the U 5f PSW, such as the resonating U 6d emission [26] and the *surface* U 5f emission [30, 31]. However, the resonating U 6d intensity would be weak [32][5]. Further, it is likely that the resonating U 6d intensity is normalized out in subtracting the off-resonance spectrum from the on-resonance spectrum because it usually mimics the ligand d and sp density of states (DOS). The photon energies employed in this study are known to be surface-sensitive [30, 31]. The 5f emission from the *surface* U ions might contribute to the region around 2–3 eV BE, as found in Ce systems, which will then inhibit one from observing the undistorted *bulk* electronic structure. However, in contrast to Ce systems for which the surface effects have been well established, the surface effects for uranium intermetallic compounds have not been observed explicitly at the U 4d absorption edge ($h\nu \approx 736$ eV) or at higher $h\nu$'s [28]. One possibility might be that the overall valence-band PES spectra of the U 5f *surface* states are very similar to the U 5f *bulk* PES spectra, even though its validity has not been confirmed experimentally yet.

The similarity in the U 5f PSW between UNiSn and UPdSn suggests that the interaction between U 5f electrons in UTSn (T = Ni, Pd) is mediated mainly by the hybridization to conduction-band electrons, rather than by the direct f–f hopping[6], as explained below. The average U–U separation d_{U-U} in UPdSn (3.63 Å) is much shorter than that in UNiSn (4.53 Å), but is closer to that in UAl_2 (3.22 Å). $d_{U-U} = 3.63$ Å in UPdSn lies on the border of the Hill limit ($d_{Hill} = 3.3$–3.5 Å) [33], beyond which the U 5f electrons are observed to form local moments. If we consider the average U–U separation only, the direct f–f hopping among U 5f electrons is expected to occur in UPdSn (even if it may be weak), while it is expected to be negligible in UNiSn. Thus the interaction between U 5f electrons in UTSn should be mediated by the hybridization to conduction-band electrons, such as U 6d, Sn sp and T d electrons. This conclusion is consistent with the fact that UNiSn and UPdSn have significantly larger ordered magnetic moments than in other U intermetallic systems [3, 4]. The inelastic neutron scattering study also found well-defined CEF excitations in UTSn (T = Ni, Pd) [11].

Figure 2(b) compares the $h\nu = 92$ eV off-resonance spectra of UNiSn and UPdSn, which can be considered to represent the experimental Ni 3d and Pd 4d PSWs, respectively. To find a correlation between the U 5f PSW and the hybridization effect, we compare the off-resonance spectrum ($h\nu = 92$ eV) of UAl_2 for which $N_f(E_F)$ is very large. The spectrum for UAl_2 is reproduced from [28] and it is scaled so that the area between E_F and ∼5 eV BE is comparable to that in UNiSn. It is shown that the Pd 4d peak lies at a higher BE (∼4 eV BE) than the Ni 3d peak (∼2 eV BE) and its FWHM (∼2 eV) is much wider than that of the Ni 3d peak (∼1 eV). The latter difference reflects the less localized nature of Pd 4d states than Ni 3d

[5] In this paper, the resonating Ce 5d intensity in CeNiSn is estimated to be less than 15% of the resonating Ce 4f intensity. The resonance effect of the U 6d electrons due to the U 5d → 5f RPES will be weaker than that of the Ce 5d electrons due to the Ce 3d → 4f RPES since U 5f electrons are less localized than Ce 4f electrons.

[6] The U–Ni separation (2.77 Å) and the U–Pd separation (2.92 Å) are much smaller than the U–U separations.

states. Then the more spread wavefunctions of the Pd d electrons than those of the Ni 3d electrons would yield the larger spatial overlap between U 5f and Pd 4d wavefunctions. On the other hand, due to higher BEs of the Pd 4d states, the energy overlap between U 5f and Pd 4d wavefunctions would be smaller than that between U 5f and Ni 3d wavefunctions so as to weaken the hybridization. It is thus expected that the effective hybridization in UNiSn and UPdSn becomes more or less similar to produce the similar shapes of U 5f PSWs.

Note that both the Pd 4d and Ni 3d PSWs reveal a very low spectral intensity near E_F, $I(E_F)$, which is of comparable magnitude if the main d peaks are scaled at their maxima. In contrast, UAl_2 reveals a much larger $I(E_F)$ than UTSn. This difference indicates that the reduced $N_f(E_F)$ in UTSn arises from the energy-dependent hybridization matrix elements $M_{fd}(E)$ between the U 5f states and the T d states that have a very low DOS at E_F. This interpretation implies that the energy-dependent hybridization, instead of the average hybridization strength, plays an important role in determining $N_f(E_F)$ in uranium compounds. This interpretation is consistent with that for CeMX (M = Pd, Pt; X = P, As, Sb) [34] and $CeCu_2Si_2$ [35], in which it was found to be crucial to properly consider the energy dependence of the hybridization matrix $\rho V^2(E)$ in describing the measured Ce 4f spectra using the impurity Anderson Hamiltonian. The analogy of the energy-dependent hybridization between the uranium system and the Ce system might be too naive, since Ce 4f electrons are more localized than U 5f electrons. In order to check the role of the hybridization interactions in UTSn, it is necessary to calculate the energy-dependent hybridization matrix elements $M_{fd}(E)$ between U 5f and T d states and $M_{fp}(E)$ between U 5f and Sn p states.

3.2. High-resolution PES across phase transitions

Figure 3 shows the high-resolution PES spectra of UTSn (T = Ni, Pd) in the vicinity of E_F, obtained at $h\nu = 22$ eV with FWHM $\approx$ 30 meV. All the spectra were obtained with the same measurement conditions except for temperature. The top and middle spectra show the high-resolution PES spectra of Pt metal and UTSn (T = Ni, Pd), which were obtained with $T = 15$ K, $h\nu = 22$ eV and FWHM $\approx$ 30 meV. Pt is chosen as representing the typical metallic Fermi-edge spectrum. Note that the high-resolution PES spectra of UTSn in the vicinity of E_F are almost identical to each other and that there is certainly a finite metallic DOS at E_F. On the other hand, the slope of the PES spectrum of UTSn just below E_F is lower than that of Pt, indicating a lower DOS at E_F.

We have analysed the line shapes of the high-resolution PES spectra using the model DOS. The dotted line superposed on the measured spectrum of Pt metal is the linearly flat DOS (the simple linear metallic DOS) with a non-zero slope. Similarly, the dotted line superposed on the measured spectra of UTSn is the V-shaped metallic DOS. The V-shaped metallic DOS represents a model with a reduced but finite DOS at E_F which is usually formed in semi-metallic systems, whereas the former flat DOS is formed in normal metal. Then the solid lines along the measured spectra of Pt and UTSn are the results of these models, respectively, which are cut-off at E_F by the 15 K Fermi distribution function, and convoluted with a Gaussian function with FWHM = 30 meV. It is clearly shown that each of these DOS models fit the PES spectra of Pt and UTSn very well. In contrast to a simple linear metallic DOS for Pt, the spectra for UTSn are described well by the V-shaped metallic DOS near E_F. This difference confirms that UTSn has a lower DOS at E_F than a typical metal, in agreement with a low $N_f(E_F)$ (see figure 2).

The bottom spectra present the T-dependence of the spectra of UPdSn, by comparing the spectra obtained at $T = 15$ K (black curves), the monoclinic AF phase, at $T = 30$ K (grey curves), the orthorhombic AF phase, and at $T = 60$ K (open dots), the paramagnetic phase.

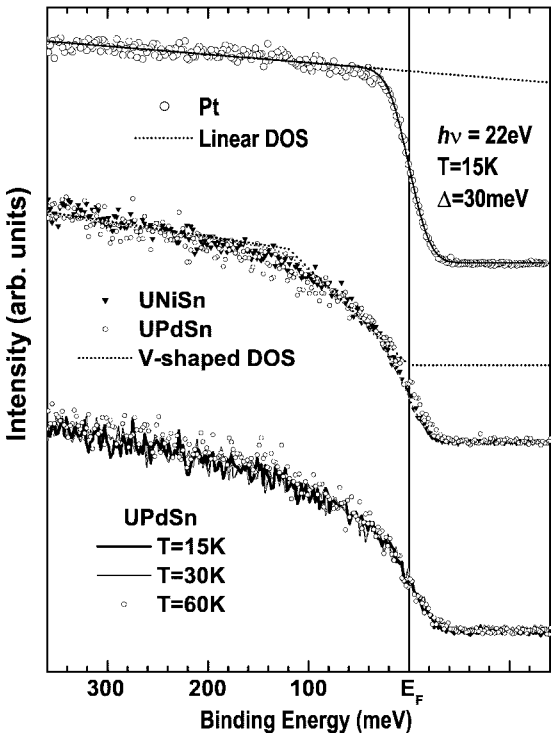

Figure 3. Top: the high-resolution photoemission spectrum of Pt metal in the vicinity of E_F, obtained at $T = 15$ K with FWHM $\approx$ 30 meV. Middle: comparison of high-resolution photoemission spectra of UTSn (T = Ni, Pd) in the vicinity of E_F, obtained at $T = 15$ K with FWHM $\approx$ 30 meV. The dotted and solid lines along Pt and UTSn are the model DOSs (see text for details). Bottom: comparison of the $h\nu = 22$ eV spectra of UPdSn obtained at $T = 15$ K (black curve), $T = 30$ K (grey curve) and $T = 60$ K (open circles).

Practically no changes have been observed in the PES spectra of UPdSn across magnetic phase transitions, except those due to temperature broadening. This finding is similar to that for UNiSn [20], where a finite DOS at E_F was observed both below and above T_N, with no noticeable changes with varying temperature. Therefore the same V-shaped metallic DOS [39] is expected to provide a reasonably good fit to the measured spectra of UPdSn at 30 and 60 K. Our study indicates that both UNiSn and UPdSn have finite metallic DOSs at E_F in different magnetic phases, suggesting that there are no appreciable changes in their electronic structures across the magnetic phase transitions. Note, however, that the $h\nu$'s employed in this study are surface sensitive (see the discussion in figure 2(a)). If the *surface* layers do not go through the SM phase transition with varying temperature, then the *surface* emission might have smeared out the changes that occur in the *bulk* electronic states near E_F with varying temperature. This might explain the missing phase transition in the PES spectrum of UPdSn.

3.3. Comparison to the LSDA + U calculation

We previously found that the LSDA calculation for UNiSn shows a large discrepancy with the measured PES spectra [20]. The most pronounced discrepancy was that the calculated peak positions in the Ni d and Sn p PDOS appear at higher BEs than in the PES spectra by more than 0.5 eV, while the calculated U 5f PDOS is concentrated within 0.5 eV of E_F, so that the

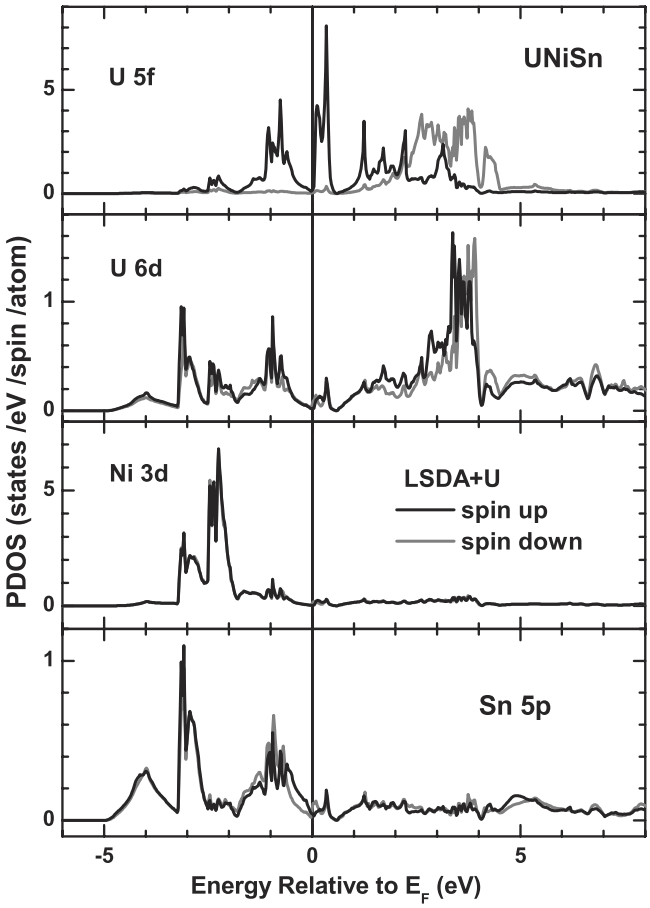

Figure 4. The calculated PDOS per spin and per atom of UNiSn, obtained from the LSDA + U calculation for the AF ground state. The spin-up and spin-down PDOS are denoted with black and grey curves, respectively. From the top are shown U 5f, U 6d, Ni d and Sn 5p PDOS.

measured 5f PSW reveals extra intensity between ∼0.5 eV to about 3 eV BE, as compared to the LSDA calculation. Therefore in order to include the effect of the electron–electron correlation between U 5f electrons in UTSn, we have performed the LSDA + U calculations for both UNiSn and UPdSn. Figures 4 and 5 show the calculated PDOS per atom of UNiSn and UPdSn, respectively, obtained from the LSDA + U calculations. Tetragonal and orthorhombic (phase I) AF structures were considered for UNiSn and UPdSn, respectively, and the collinear spin configurations of U 5f magnetic moments were assumed for both systems. As mentioned in the introduction, AF structures in UPdSn are reported to be noncollinear. We, however, expect that the local electronic structures of U sites are similar between the noncollinear and collinear spin configurations. Indeed we have obtained nearly the same electronic structures as those obtained from the noncollinear spin configurations calculation [17], as discussed below. The on-site Coulomb correlation parameter U for the U 5f electrons was included in these calculations. The parameters used in these calculations were the Coulomb correlation $U = 2.0$ eV and the exchange $J = 0.95$ and 0.8 eV for UNiSn and UPdSn, respectively. We employed the above U value from the existing LSDA + U calculations [15, 36, 37] for

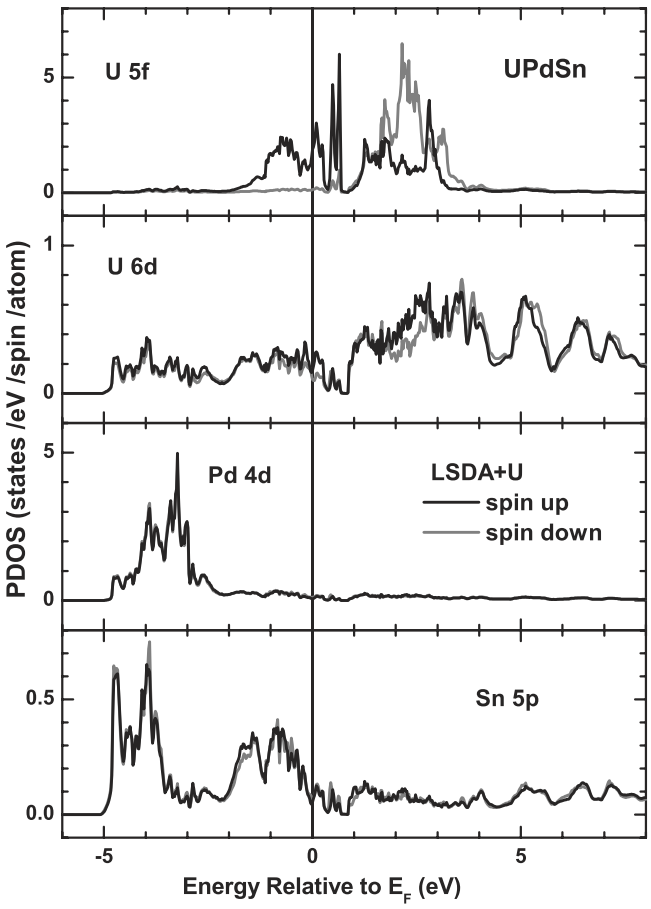

Figure 5. The calculated PDOS per spin and per atom of UPdSn, obtained from the LSDA + U for the AF ground state.

several uranium systems, which yields the electronic structures in good agreement with the experiments. The on-site Coulomb correlations for Ni 3d and Pd 4d electrons were neglected. The LSDA + U yields the correct metallic ground states for the AF phase of UTSn (T = Ni, Pd), and the correct semiconducting and metallic ground states for the paramagnetic phases of UNiSn and UPdSn, respectively. These theoretical results are qualitatively similar to those of previous reports [15, 17]. Note that the AF phase of UNiSn has the normal metallic electronic structure in contrast to the half-metallic electronic structure for the ferromagnetic phase [16].

The major effect of including U in the LSDA + U is to shift both the occupied 5f peaks and the unoccupied 5f peaks away from E_F [20]. The second effect of the LSDA + U is to shift the U d, T d, and Sn p PDOS toward E_F. The larger the U value is, the larger the peak shift becomes. The calculated specific-heat coefficient γ values are 5.5 and 7.3 mJ mol^{-1} K^{-2} for UNiSn and UPdSn, respectively. The calculated γ value for UNiSn is smaller than the experimental value, but that for UPdSn agrees reasonably well with experiment [1, 2], reflecting that the contribution from phonons or spin fluctuations would be larger for UNiSn than for UPdSn. For UTSn (T = Ni, Pd), the calculated orbital and spin magnetic moments for U ions are 4.53 and $-2.25\ \mu_B$ (UNiSn), and 4.53 and $-2.24\ \mu_B$ (UPdSn), respectively, and so the total

magnetic moments of U ions become 2.28 μ_B (UNiSn) and 2.29 μ_B (UPdSn). These values are in reasonable agreement with experiment [3, 4]. The total magnetic moment 2.29 μ_B for UPdSn is also in reasonable agreement with the value 2.01 μ_B obtained from the noncollinear spin configuration calculation [17]. The calculated spin magnetic moments of U 5f states, $\sim$2 μ_B for both UNiSn and UPdSn, reflect that the number of the occupied 5f electrons is close to two ($5f^2$) with U^{4+} configuration. Note, however, that 5f electrons in UNiSn and UPdSn are not so localized as in UPd_3 due to the large hybridization with the neighbouring elements. Therefore the f-electron count is not really meaningful in these intermetallic compounds.

For both UNiSn and UPdSn, the U f states exhibit the exchange-split 5f bands, separated from each other by about 4 and 3 eV, respectively. The other states (U d, T d, Sn p) exhibit nearly no exchange splitting, indicating that the spin-polarization in UTSn is mainly due to the U f electrons. The Ni and Pd d bands are nearly filled with a very low DOS at E_F, in agreement with the PES data (see figure 2). The Sn p states are spread over the whole valence band, but relatively more concentrated at 1–2 eV below E_F. The U d, T d and Sn p PDOS share common features, indicating the large hybridization among them. The f PDOS at E_F is low for UNiSn, but high for UPdSn. It is because that the Fermi level in UNiSn cuts the valley of U f DOS, while the Fermi level in UPdSn is located near the second peak of the U f DOS. This difference arises from the different crystal structures of UNiSn and UNiSn.

Figure 6 compares the extracted PSWs (dots) of UTSn (T = Ni, Pd) to the calculated PDOS, obtained from the LSDA + U calculations (solid curves). In the comparison to the PES spectra, only the occupied parts of the calculated PDOS were taken, and then convoluted by a Gaussian function with 0.2 eV at the FWHM. The Gaussian function was used to simulate the instrumental resolution. The effects of the lifetime broadening and the photoemission matrix elements were not included in the theory curves [38][7]. At the bottom panels, the theoretical spectra correspond to the sum of the U d, T d and Sn p PDOS, because none of the contributions are negligible at $h\nu = 22$ eV and it is difficult to separate them out (see the discussion under figure 1).

The LSDA + U calculation provides reasonably good agreement with PES for UPdSn, but not for UNiSn. The calculated U 5f PDOS for UPdSn shows a metallic DOS at E_F, resulting in good agreement with PES. The nearly negligible DOS at E_F for T d states (T = Ni, Pd) in the LSDA + U calculations gives good agreement with PES. For UPdSn, the peak positions in the LSDA + U agree very well with the PES spectra for Pd d and Sn sp states. In contrast, the calculated peak positions in UNiSn appear at slightly higher BEs than in the PES spectra. In particular, the calculated U f peaks in the occupied part appear at higher BEs than in PES, and the calculated $N_f(E_F)$ is too small, as compared to PES. It is surprising that the LSDA + U calculation for UPdSn gives good agreement with the measured U 5f PES, whereas that for UNiSn does not. This finding indicates that the U 5f electronic structure for UPdSn is described well by the band structure calculations when the small on-site Coulomb interaction for U 5f electrons is included. It is likely that the differences between UNiSn and UPdSn arise from the more localized nature of Ni 3d electrons, as compared to Pd 4d electrons, and their structural differences. These differences seem to affect the nature of U 5f electrons, probably via the different hybridization effect between T d and U 5f electrons. In examining the nature of the U 5f electrons in UNiSn, a more precise experiment is required, such as high-resolution angle-resolved PES near the U 5f RPES region for single crystalline samples, to search for a possible dispersion of the U 5f states.

[7] The calculated photoemission matrix elements for some uranium systems have been reported, showing that they depend on the incident photon energy and the kinetic energy of the outgoing electrons (see [38]). The calculated photoemission matrix elements exhibit the non-linear kinetic energy dependence.

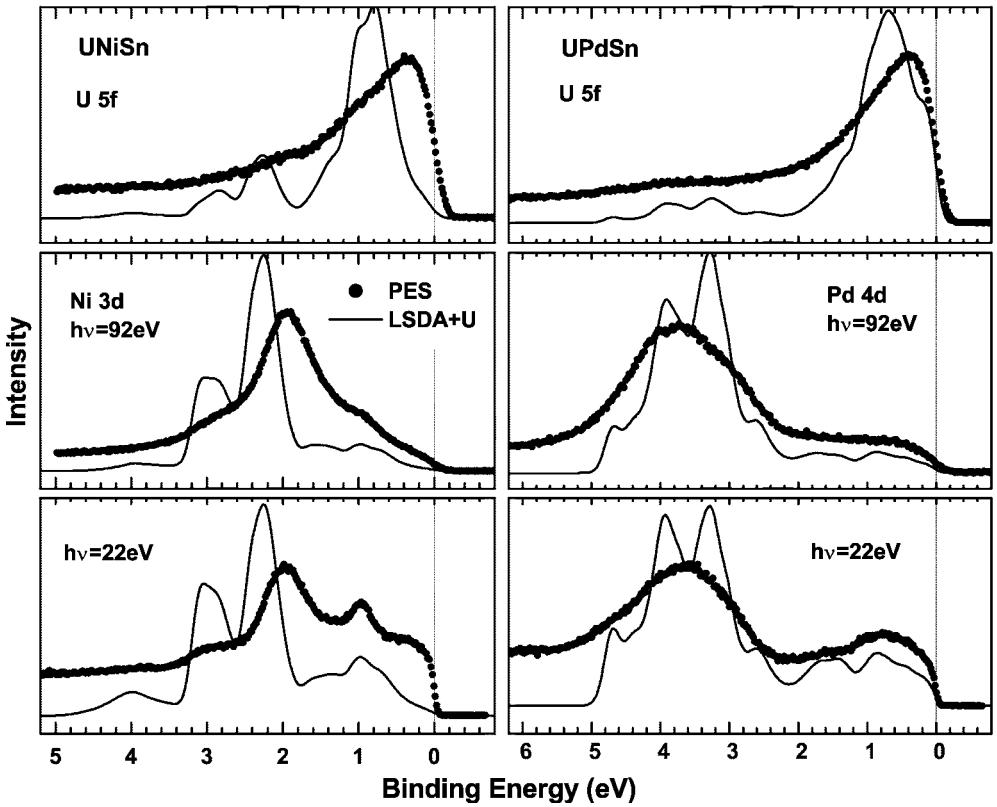

Figure 6. Top: comparison of the extracted U 5f PSW (dots) of UNiSn (left) and UPdSn (right) to the calculated PDOS, obtained from the LSDA + U calculation (solid curve). Middle: similarly for Ni 3d and Pd 4d states. Bottom: comparison of the $h\nu = 22$ eV PES spectrum of UTSn (dots) to the sum of the U 6d, T d and Sn 5p PDOS. See the text for details.

4. Conclusions

The electronic structures of UTSn (T = Ni, Pd) have been investigated by performing the photoemission experiment and the LSDA + U electronic structure calculation. The extracted U 5f spectra of UTSn are very similar to each other, showing the U 5f peaks at ≈ 0.3 eV BE. Compared to the U 5f PSWs of a nearly heavy fermion system UAl_2 and a typically localized 5f system UPd_3, the centroid of the 5f electron peak moves away from E_F from UAl_2 to UTSn and UPd_3, accompanied by the decreasing 5f spectral weight at the Fermi level, $N_f(E_F)$, which suggests that the extent of the localization of U 5f electrons in UTSn is in between UAl_2 and UPd_3. The similarity in the U 5f PSW between UNiSn and UPdSn suggests that the interaction between U 5f electrons in UTSn is mediated mainly by the hybridization to conduction-band electrons, rather than by direct f–f hopping. Both the Ni 3d and Pd 4d PSWs show the main peaks well below E_F and a very low DOS at E_F.

The high-resolution PES spectra of UTSn are also very similar each other, with the slope just below E_F being lower than that of a typical metal. They are described well by a V-shaped metallic DOS near E_F, consistent with the reduced 5f DOS at E_F. The temperature-dependent high-resolution PES spectra of UTSn manifest no noticeable changes in their electronic structures across the magnetic phase transition temperatures. Both the high-resolution PES

and the T d PSWs suggest that the reduced $N_f(E_F)$ in UTSn is ascribed to the hybridization to the very low T d DOS at E_F. This conclusion implies that the energy-dependent hybridization is operative in determining the U 5f electronic structure. Comparison of the measured PES spectra to the LSDA + U band structure calculation reveals reasonably good agreement for UPdSn, but not for UNiSn. The calculated spin magnetic moments of U 5f states, $\sim 2\ \mu_B$ for both UNiSn and UPdSn, reflect that the number of the occupied 5f electrons is close to two ($5f^2$) with the U^{4+} configuration. The present work suggests that the U 5f electronic structure in UPdSn is described well by the band structure calculations by including the small on-site Coulomb interaction for U 5f electrons, which supports the less localized nature of U 5f electrons in UPdSn than in UNiSn.

Acknowledgments

This work was supported by the KRF (Grant No. KRF–2002-070-C00038), by the KOSEF through the CSCMR at SNU and the eSSC at POSTECH, and in part by the Research Fund, 2004, of the Catholic University of Korea. The SRC is supported by the NSF (DMR-0084402).

References

[1] Palstra T T M, Nieuwenhuys G J, Vlastuin R F M, van den Berg J, Mydosh J A and Buschow K H J 1987 *J. Magn. Magn. Mater.* **67** 331
[2] de Boer F R, Brück E, Nakotte H, Andreev A V, Sechovsky V, Havela L, Nozar P, Denissen C J M, Buschow K H J, Vaziri B, Meissner M, Maletta H and Rogl P 1992 *Physica* B **176** 275
[3] Kawanaka H, Fujii H, Nishi M, Takabatake T, Motoya K, Uwatoko Y and Ito Y 1989 *J. Phys. Soc. Japan* **58** 3481
[4] Robinson R A, Lawson A C, Buschow K H J, de Boer F R, Sechovsky V and Von Dreele R B 1991 *J. Magn. Magn. Mater.* **98** 147
Robinson R A, Lawson A C, Lynn J W and Buschow K H J 1992 *Phys. Rev.* B **45** 2939
[5] Akazawa T, Suzuki T, Nakamura F, Fujita T, Takabatake T and Fujii H 1996 *J. Phys. Soc. Japan* **65** 3661
[6] Fujii H, Kawanaka H, Takabatake T, Kurisu M, Yamaguchi Y, Sakurai J, Fujiwara H, Fujita T and Oguro I 1989 *J. Phys. Soc. Japan* **58** 2495
[7] Diel J, Fischer H, Köhler R, Geibel C, Steglich F, Maeda Y, Takabatake T and Fujii H 1993 *Physica* B **186–188** 708
[8] Nakotte H, Robinson R A, Purwanto A, Tun Z, Prokes K, Brück E and de Boer F R 1998 *Phys. Rev.* B **58** 9269
[9] Aoki Y, Suzuki T, Fujita T, Kawanaka H, Takabatake T and Fujii H 1993 *Phys. Rev.* B **47** 15060
[10] Akazawa T, Suzuki T, Goshima H, Tahara T, Fujita T, Takabatake T and Fujii H 1998 *J. Phys. Soc. Japan* **67** 3256
Akazawa T, Suzuki T, Tahara T, Goto T, Hori J, Goshima H, Nakamura F, Fujita T, Takabatake T and Fujii H 1999 *Physica* B **259–261** 248
[11] McEwen K A, Bull M J and Eccleston R S 2000 *Physica* B **281/282** 600
[12] Johnson S W, Robinson R A, Nakotte H, Bruck E, de Boer F R and Larson A C 1993 *J. Appl. Phys.* **73** 6072
[13] Paixao J A, Robinson R A, Lander G H and Brown P J 1999 *J. Phys.: Condens. Matter* **11** 2127
[14] Trygg J, Johansson B and Eriksson O 1994 *Phys. Rev.* B **49** 7165
[15] Oppeneer P M, Yaresko A N, Perlov A Ya, Antonov V N and Eschrig H 1996 *Phys. Rev.* B **54** R3706
[16] Albers R C, Boring A M, Daalderop G H I and Mueller F M 1987 *Phys. Rev.* B **36** 3661
[17] Sandratskii L M and Kübler J 1997 *J. Phys.: Condens. Matter* **9** 4897
[18] Höchst H, Tan K and Buschow K H J 1986 *J. Magn. Magn. Mater.* **54–57** 545
[19] Havela L, Almeida T, Naggele J R, Sechovsky V and Brück E 1992 *J. Alloys Compounds* **181** 205
Havela L, Sechovsky V, Naggele J R, Almeida T, Brück E H, Nakotte H and de Boer F R 1992 *J. Magn. Magn. Mater.* **104–107** 23
[20] Kang J-S, Park J-G, McEwen K A, Olson C G, Kwon S K and Min B I 2001 *Phys. Rev.* B **64** 085101
[21] Anisimov V I, Aryasetiawan F and Liechtenstein A I 1997 *J. Phys.: Condens. Matter* **9** 767
[22] Kwon S K and Min B I 2000 *Phys. Rev. Lett.* **84** 3970
[23] Yeh J J and Lindau I 1985 *At. Data Nucl. Data Tables* **32** 1

[24] Arko A J, Koelling D D and Reihl B 1983 *Phys. Rev.* B **27** 3955
[25] Landgren G, Jugnet Y, Morar J F, Arko A J, Fisk Z, Smith J L, Ott H R and Reihl B 1984 *Phys. Rev.* B **29** 493
[26] Arko A J, Koelling D D, Capasso C, del Giudice M and Olson C G 1988 *Phys. Rev.* B **38** 1627
[27] Kang J-S, Allen J W, Maple M B, Torikachvili M S, Ellis W P, Pate B B, Shen Z-X, Yeh J J and Lindau I 1989 *Phys. Rev.* B **39** 13529
[28] Allen J W, Zhang Y-X, Theng L H, Cox L E, Maple M B and Chen C-T 1996 *J. Electron. Spectrosc. Relat. Phenom.* **78** 57
[29] Frings P H and Franse J J M 1985 *Phys. Rev.* B **31** 4355
[30] Duo L 1998 *Surf. Sci. Rep.* **32** 233
[31] Sekiyama A, Iwasaki T, Matsuda K, Saitoh Y, Onuki Y and Suga S 2000 *Nature* **403** 398
[32] Sekiyama A, Suga S, Iwasaki T, Ueda S, Imada S, Saitoh Y, Yoshino T, Adroja D T and Takabatake T 2001 *J. Electron. Spectrosc. Relat. Phenom.* **114–116** 699
[33] Hill H H 1970 Plutonium 1970 and Other Actinides *Nucl. Met.* vol 17, ed W N Miner (New York: Metallurgical Society of AIME) pp 2–19
[34] Iwasaki T, Sekiyama A, Yamasaki A, Okazaki M, Kadono K, Utsunomiya H, Imada S, Saitoh Y, Muro T, Matsushita T, Harima H, Yoshii S, Kasaya M, Ochiai A, Oguchi T, Katoh K, Niide Y, Takegahara T and Suga S 2002 *Phys. Rev.* B **65** 195109
[35] Kang J-S, Allen J W, Gunnarsson O, Christensen N E, Andersen O K, Lassailly Y, Maple M B and Torikachvili M S 1990 *Phys. Rev.* B **41** 6610
[36] Brooks M S S, Johansson B, Eriksson O and Skriver H L 1986 *Physica* B **144** 1
[37] Severin L, Brooks M S S and Johansson B 1993 *Phys. Rev. Lett.* **71** 3214
[38] Marksteiner P *et al* 1986 *Phys. Rev.* B **34** 6730
Boring A M *et al* 1987 *Phys. Rev.* B **35** 2447
[39] Kang J-S, Park J-G, McEwen K A, Ōnuki Y, Olson C G and Min B I 2002 *Physica* B **312/313** 882